



Published in final edited form as:

DNA Repair (Amst). 2008 February 1; 7(2): 253–266.

## Brca1 in immunoglobulin gene conversion and somatic hypermutation

Simonne Longerich<sup>a</sup>, Brian Orelli<sup>b</sup>, Richard Martin<sup>b</sup>, Douglas Bishop<sup>c</sup>, and Ursula Storb<sup>a,b,\*</sup>

<sup>a</sup>Committee on Immunology, University of Chicago, Chicago, IL 60637

<sup>b</sup>Department of Molecular Genetics and Cell Biology, University of Chicago, Chicago, IL 60637

<sup>c</sup>Department of Radiation and Cellular Oncology, University of Chicago, Chicago, IL 60637

### Abstract

Defects in *Brca1* confer susceptibility to breast cancer and genomic instability indicative of aberrant repair of DNA breaks. *Brca1* was previously implicated in the homologous recombination pathway via effects on the assembly of recombinase Rad51. Activation-induced cytidine deaminase (AID) deaminates C to U in B lymphocyte immunoglobulin (*Ig*) DNA to initiate programmed DNA breaks. Subsequent Uracil-glycosylase mediated U removal, and perhaps further processing, leads to four known classes of mutation: *Ig* class switch recombination that results in a region-specific genomic deletion, *Ig* somatic hypermutation that introduces point mutations in *Ig* V-regions, *Ig* gene conversion in vertebrates that possess *Ig* pseudo-V genes, and translocations common to B cell lymphomas. We tested the involvement of *Brca1* in AID-dependent *Ig* diversification in chicken DT40 cells. The DT40 cell line diversifies *Ig* *V $\lambda$*  mainly by gene conversion, and less so by point mutation. *Brca1*-deficiency caused a shift in *V $\lambda$*  diversification, significantly reducing the proportion of gene conversions relative to point mutations. Thus, *Brca1* regulates AID-dependent DNA lesion repair. Interestingly, while *Brca1* is required to recruit ubiquitinated FancD2 to DNA damage, the phenotype of *Brca1*-deficient DT40 differs from the one of FancD2-deficient DT40, in which both gene conversion and non-templated mutations are impaired.

### 1. Introduction

Fundamental to humoral immunity is the vast diversity and exquisite specificity of antibodies. During early B cell development, germline immunoglobulin (*Ig*) *V*, *D* and *J* gene segments recombine to generate unique antibody variable region exons (combinatorial diversity). In humans and mice, immense diversity is generated from the possibly limitless combinations of *V(D)J* segments. Functional, assembled *Ig* genes are diversified further by three mechanisms: somatic hypermutation introduces point mutations and occasional insertions and deletions into the assembled *V(D)J* exon and flanks with the purpose to increase the affinity of antigen-specific antibodies. Alternatively, in chickens and a few other vertebrates where a small number of functional *V* gene segments limits combinatorial diversity (eg., in chickens only single functional *V* and *J* genes at L and H chain loci rearrange [1], further diversification is accomplished by gene conversion (GC) between the active *V* exon and a collection of 5' pseudo-*V* gene segments [2,3]. GCs are characterized by mutations in the active *V* gene derived in sequence tracts of variable length from pseudo-*V* gene donor sequences during homologous

\* Corresponding author: Tel. 773-702-4440, Fax. 773-702-3172, Email stor@uchicago.edu.

**Publisher's Disclaimer:** This is a PDF file of an unedited manuscript that has been accepted for publication. As a service to our customers we are providing this early version of the manuscript. The manuscript will undergo copyediting, typesetting, and review of the resulting proof before it is published in its final citable form. Please note that during the production process errors may be discovered which could affect the content, and all legal disclaimers that apply to the journal pertain.

recombination. Third, the Ig constant region isotype is altered by class switch recombination (CSR). CSR targets a genomic deletion that fuses a non-IgM/D constant region to the variable region.

SHM, GC and CSR share in common the requirement for activation-induced deaminase (AID), expression of which is strongly and specifically induced in activated B cells and chicken bursal B cells undergoing GC [4,5]. AID deaminates cytosine bases in *Ig* genes to produce uracils; untouched, the resulting U-G mismatches lead to transition mutations from G and C (ie., C to T and G to A) [6,7]. Alternatively, the uracil glycosylase Ung and mismatch repair enzymes Msh2/6 initiate further processing of the U-G mismatch to produce DNA breaks that lead to SHM, CSR, or GC by a regulated mechanism that is not understood (reviewed by [8]). Regulation of AID-mediated genomic alterations indeed is crucial because dysregulated AID expression and/or absence of DNA repair proteins involved in regulating the outcome of an AID-induced DNA lesion lead to oncogenic translocations of types frequently observed in lymphomas [9].

The chicken bursal B cell line DT40 constitutively acquires AID-dependent *Ig* GCs and SHM-like point mutations in the rearranged *V $\lambda$*  allele [10] and has become a popular model system for analyzing the genetic requirements for GC and SHM (as well as other processes) because of the relative ease of generating gene-knockout lines [11]. Moreover, genetic changes at the *Ig* heavy and  $\lambda$  light chain loci can be monitored phenotypically by gain or loss of surface IgM [12]. For example, the popular CL18 line of DT40 harbors a frameshift mutation in *V $\lambda$*  that abolishes surface IgM expression; the frameshift can be corrected by homologous recombination/GC with one of several *V $\lambda$*  pseudogenes to restore surface IgM. Homologous recombination in vertebrates is catalyzed by Rad51. Like bacterial RecA, Rad51 polymerizes on single-stranded DNA to form nucleoprotein filaments that catalyze pairing and strand exchange with homologous DNA (reviewed by [13]). Both in mammals and DT40, *Rad51* is an essential gene [14]. However, DT40 cells deficient for any of the five vertebrate *Rad51* paralogs (*Rad51B*, *Rad51C*, *Rad51D*, *XRCC2* and *XRCC3*, which in humans share 20-30% identity with *Rad51*) are viable though impaired for homologous recombination, and all display a decrease in the frequency of *Ig* GC, as expected. Impaired *Ig* GC also is observed in DT40 cells mutated in *BRCA2*, a breast cancer susceptibility gene whose encoded protein plays a direct role in regulating Rad51 [15]. Surprisingly however, all *Rad51* paralog, and *BRCA2* mutants also display a concomitant increase in the frequency of point mutations in *V $\lambda$*  [15], a phenotype also achieved by deletion of the  $\lambda$  pseudo-*V* genes (ie., GC donor sequences) [16]. Together these results suggest that preventing recombination by absence of either the enzymes that catalyze recombination, or the recombination donor DNA, results in accumulation of *V $\lambda$*  point mutations that resemble mammalian SHM.

Ung-deficient DT40 also fail to perform GC but uniquely accumulate G/C transition mutations in *Ig* genes because they fail to remove AID-deaminated cytosines [6,17]. In contrast, DT40 cells lacking Rev1 (a dCMP transferase, and an adapter protein for error-prone polymerases Pol $\eta$ , Pol $\iota$ , Pol $\kappa$ , and Pol $\zeta$ , [18]) generate GCs almost exclusively, indicating that Rev1 is necessary for generating SHM-like point mutations [19,20]. These results imply that a common intermediate – a U/G mismatch generated by AID, processed into a single-strand gap by Ung and subsequent base excision repair enzymes, and perhaps further processing (for instance by the Mre11-Rad50-NbsI endonuclease complex, [21]) – initiates SHM or GC depending on the availability of partially homologous V-region donor sequence in *cis*, and the DNA repair factors involved [22].

Both *Brca2* and *Brca1* proteins are involved in DNA repair. Defects in either protein confer susceptibility to breast cancer [23], and genomic instability characterized by spontaneous accumulation of chromosomal rearrangements including translocations, deletions and

chromosome fusions that indicate aberrant repair of DNA breaks (reviewed by [24]). Unlike Brca2 which binds Rad51 directly, it is not yet clear whether Brca1 interaction with Rad51 is direct or indirect. Nevertheless, Brca1 is involved in homologous recombination (reviewed by [25]; formation of ionizing radiation- and cisplatin-induced Rad51 nuclear foci require Brca1 in mammalian cells and DT40 [26-28], and homologous recombination repair of double-strand breaks is impaired in Brca1-deficient cells [29,30]. However, Brca1 also is reported to function in other DNA repair pathways, and diverse processes including transcription and cell cycle control (reviewed by [13,24]. Moreover, Brca1 is reported to interact with a large number of proteins, of which not all are implicated in DNA repair. In most cases, the functional significance of the Brca1 interaction is unclear, as is the function of Brca1 itself (reviewed by [31]. However, a number of the proteins with which Brca1 interacts are involved in Ig GC and/or SHM, including Brca2 [32], the Mre11/Nbs1/Rad50 complex [33], Msh2/6 [34] and FancD2 [35]. Notably, DNA damage-localized Brca1 recruits FancD2, one of 13 proteins defective in Fanconi anemia, and which function in DNA repair (reviewed by [36]. Intriguingly, DT40 cells defective in FancD2 and FancC are impaired for both Ig GC as well as non-templated mutation [35,37].

We asked whether Brca1 plays a role in regulating Ig GC and non-templated point mutation in DT40. We hypothesized that Brca1-deficient DT40 might be impaired for Ig GC if Brca1 plays a role in facilitating GC, and further, that Brca1-deficient cells would lack non-templated mutations if Brca1 is epistatic to FancD2.

## 2. Materials and methods

### 2.1. DT40 cell lines and culture

The parent of the *Brca1*<sup>-/-</sup> cells (Fig.1) was DT40 *cre*. It and AID<sup>-/-</sup> derivatives were a gift from J.-M. Buerstedde and H. Arakawa (Institute of Molecular Radiobiology, GSF, Munich, Germany) via M. Nussenzweig and N. Papavasiliou (Rockefeller U., New York). DT40 *cre*, a derivative of CL18, expresses a *v-myb* transgene and also is transgenic for tamoxifen-inducible Cre recombinase [38]. Presumably due to *v-myb* expression, DT40 *cre* performs GC at a ~5-fold increased rate in comparison to the DT40 parent line [38]. The parent of the *Brca1*<sup>-/-</sup> (clone #8) and the *Brca1*<sup>-/-</sup> (“partial” clone #37) lines is an IgM<sup>+</sup> derivative of CL18 [39]. This DT40 cell line does not contain a *v-myb* or Cre transgene. The *Brca1*<sup>-r</sup> lines (clones C1, F10 and L4) are the result of homologous integration of a chicken *Brca1* cDNA (with the first two introns retained to promote efficient expression regulated by mRNA splicing) into one allele of the *Brca1*<sup>-/-</sup> “partial” line (O. Yildiz, Y. Li, and D. B., unpublished). CL18 and the *XRCC3*<sup>-/-</sup> derivative thereof were generously provided by S. Takeda (Japan). CL18 and derivatives are mostly IgM<sup>-</sup>, due to a frameshift in *V $\lambda$*  [12]. All cells were cultured in RPMI supplemented with L-glutamine, 10% FBS, 1% chicken serum (Sigma), penicillin/streptomycin, and  $\beta$ -mercaptoethanol. Cells were cultured at 39.5°C, 5% CO<sub>2</sub>.

### 2.2. Transfection and selection of DT40 cre

To obtain the *Brca1*-targeting vector with the blasticidin-resistance cassette, a histidine-resistance cassette was removed by *Bam*H1 digest of pNRB384, a *Brca1*-targeting vector (Fig. 1B), and replaced with the blasticidin-resistance cassette removed from pNRB397 by BamH1 restriction. The puromycin-resistance cassette was similarly exchanged using pNRB383. The 5' targeting flank is homologous with exons 1-2, and the 3' flank is homologous with exon 11 of chicken *Brca1*.

For transfecting DT40 *cre* by electroporation, the targeting vector was linearized with NotI. Drug selection was started 12-16 hrs after electroporation with 25  $\mu$ g/mL blasticidin (EMD Biosciences) or 0.5  $\mu$ g/mL puromycin (AG Scientific).

### 2.3. Screening of drug-resistant DT40 cre clones for targeted integration of the *Brca1* locus

One vial of 5-10 x 10<sup>6</sup> cells of each drug-resistant clone was frozen within 1-2 weeks of transfection to prevent in vitro evolution. Parallel cultures were expanded to obtain 5-10 x 10<sup>6</sup> cells that were harvested to purify DNA. Southern blots were probed with an 0.4-kb *EcoRI* fragment homologous with the chicken *Brca1* locus just 3' of the 3' targeting flank sequence, but just 5' of a diagnostic *HindIII* site (Fig. 1B).

### 2.4. Protein extraction and western blotting to detect *Brca1* protein in DT40

The "NE-PER nuclear and cytoplasmic reagents kit" (Pierce), supplemented with a protease inhibitor cocktail (Roche), NaF (1mM) and Na<sub>3</sub>VO<sub>4</sub> (1mM), consistently solubilized *Brca1* into the "nuclear," but not the "cytoplasmic" fraction (Fig. 1C). Cell lysates were resolved on 5-6% denaturing polyacrylamide mini-gels and transferred to PVDF Immobilon-P membranes (Millipore). The membranes were probed with rabbit anti *Brca1* (a gift of N. Lowndes, University of Glasgow, Scotland).

### 2.5. RT-PCR

RNA was extracted using the RNAqueous kit (Ambion). First-strand cDNA was produced using the Superscript II cDNA synthesis kit (Gibco-BRL) according to the manufacturer's directions. Negative control templates were generated by identical first-strand synthesis reactions, but without addition of reverse transcriptase. Serial dilutions of first-strand cDNA were used as template for gene-specific PCR. Gene-specific primers and PCR conditions were as follows: ggRad6F: 5' tgatgcgggactcaagagattgc, ggRad6R 5' ctgtggcacttgaaattcttgtagc; ggPCNAF 5' agggctcgggtgctcaagc; ggPCNAR 5' ctcaatcttgagccaggtag; ggActinF 5' ccccaagcttactcccacagccagccatgg; ggActinR 5' ggctctagatagtcaggtcacggcca. PCR conditions were 95°C, 4 min (1 cycle), 95°C, 30 seconds-56°C, 30 seconds-72°C, 1 minute (30 cycles) and 72°C, 7 minutes (1 cycle), using 3-fold dilutions of input first-strand cDNA.

### 2.6. Fluctuation analyses of IgM loss and gain in DT40

For each experiment, 12-24 independent cultures (derived by limiting dilution, manually or "automated" by flow sorting single cells into 96-well round-bottom plates) were first expanded to 1 mL in 24-well plates, then passaged daily for 2-6 weeks as indicated for each experiment (and determined by the doubling times for different DT40 lines; on average, 90-100 cell generations occurred in one experiment), maintaining cells at approximately 0.3-1.2 x 10<sup>6</sup> cells/mL. Cells rinsed in PBS and transferred to 96-well plates were then stained (or not, as a control) for surface IgM (with anti-chicken IgM, FITC-labeled, Bethyl Labs) in PBS 0.3% BSA, and analyzed on a FACScanII flow cytometer. 10,000-30,000 events were collected for each independent culture.

The percent of surface IgM loss in each culture was determined as described [12]; for each sample, live cells were gated on forward- and side-scatter plots, then displayed as histograms to detect FITC on the FL1 channel. For each sample, the IgM- (FITC-negative) gate boundaries were set to 8-fold below the median FL1 channel of the whole live population. The percent of cells falling within the entire IgM- gate represent the frequency of IgM loss in one culture. In a set of cultures of one genotype, the median of the IgM loss frequency was also calculated.

Genomic DNA was collected using the DNEasy kit (Qiagen) from a few clones of each set of cultures at the end of each experiment, from cells either sorted, or not, on the basis of their changed surface IgM phenotype.

## 2.7. Cloning, sequencing and mutation analysis of the DT40 V $\lambda$ locus

Analysis of events occurring at the V $\lambda$  locus in DT40 over time were performed essentially as described [12]. Briefly, genomic DNA from ~10,000 cell-equivalents was used as a template for PCR-amplification with Pfu polymerase using CVLF6 (5' CAGGAGCTCGCGGGGCCGTCAGTACTGATTGCCG 3') and CVLR3 (5' GCGCAAGCTTCCCCAGCCTGCCGCCAAGTCCAAG 3') with the following PCR cycling: 1 cycle at 94°C for 4 minutes, 9 cycles of 94°C for 1 minute, 68°C for 1 minute (decreased by 1°C every cycle and 72°C for 1.5 minutes, followed by 21-22 cycles of 94°C for 30 seconds, 60°C for 1 minute, and 72°C for 1.5 minutes, lastly extending for 7 minutes at 72°C. PCR products were cloned into pTopoII Blunt (Invitrogen) according to the manufacturer's instructions and used for transformation of *E. coli* Top10 cells. Bacterial colonies were sent for semi-automated culturing, plasmid preparation, and sequencing to the DNA core facility, University of Chicago, using M13F and M13R primers (Invitrogen).

Sequence changes in each clone were compared against a template sequence (Figure S2). Sequence changes that occurred in clones derived from the same culture were scored only once since all cells in one culture are clonally related, but if the same change occurred in multiple (but not all cultures of the same genotype – these were considered polymorphisms) cultures, the change was scored once for each independent culture. This is evident in Figure S2, where the same mutation occurred multiple times at the same nucleotide position in different subclones.

Classification of sequence changes as GCs, non-templated point mutations, or ambiguous was performed as described [12]. We used as references the sequences of the 25 known pseudo-V $\lambda$  genes [2] with modifications specific for the  $\lambda$ G4 rearranged allele (DT40 is heterozygous for the *Ig $\lambda$*  locus, the unrearranged allele being  $\lambda$ S3) as described [40]. Mutation frequencies for DT40 cre and *Brcal*-deficient derivatives were calculated as the number of mutational events (where one GC or one point mutation is one event) per number of total bps sequenced of clones not sorted for surface IgM phenotype.

## 2.6. Growth and clonogenic survival assays

Doubling times were determined by trypan blue exclusion using a Levy Brightline hemacytometer. Methylcellulose clonogenic assays were performed in 6-well plates containing DMEM-F12 (Gibco) supplemented with 7.5% FBS (Atlas), 1% chicken serum (Sigma) and 6% methyl-cellulose (Sigma). Cells were irradiated using a Maxitron generator calibrated for this purpose (250 KVp photons, 15 mA, 0.5 mm Cu filtration, dose rate=1.55 Gy/min).

## 3. Results

### 3.1. Generation of *Brcal*-deficient DT40

*Brcal*-deficient derivatives of the DT40 cre cell line were generated by targeted integration. This derivative of DT40 was chosen because it undergoes a high rate of *Ig* GC relative to the “parental” DT40 line [41]. Targeting vectors for deleting chicken *Brcal* were designed to remove a major portion of the *Brcal* coding sequence between exons two and eleven, as depicted in Fig. 1B. As assayed by Southern blotting (Fig. 1A), targeted integration efficiency for the *Brcal* locus in DT40 cre was fairly low (4/41 clones targeted to obtain the heterozygous line) in comparison to reported homologous integration frequencies in DT40 for many loci (eg., [11]), but similar low frequencies have been reported for some loci (eg., [17]). Targeting at the second allele occurred with a significantly lower frequency (3/139; P=0.048), perhaps because heterozygosity for *Brcal* reduces the efficiency of homologous integration. Homologous integration frequencies for the *Brcal* locus are summarized in Table 1. Two lines (#100 and #125) homozygous for *Brcal* disruption were analyzed for *Brcal* protein by western

blotting in parallel with DT40 cre and the *Brca1*-heterozygous intermediate (clone #28). Neither homozygous *Brca1*-disrupted line produces detectable amounts of Brca1 protein (Fig. 1C).

Compared with the DT40 cre parent, *Brca1*-deficient lines display a dose-dependent increase in cell cycle time: doubling times were 8.3, 8.5, 10.3 and 9.7 hours for DT40 cre, DT40 cre *Brca1*<sup>+/-</sup> clone 28, and DT40 cre *Brca1*<sup>-/-</sup> clones 100 and 125, respectively (Fig.S1A). In addition, both *Brca1*<sup>-/-</sup> lines are significantly more sensitive to X-ray-induced cell death (ie, at 1 Gray exposure, slightly less than 50% of cells of both *Brca1*-deficient lines survive, whereas almost 80% of the DT40 cre parent survive this dose (Fig. S1B). Both the reduced growth rate and the X-ray sensitivity phenotypes are consistent with phenotypes of *Brca1*-deficient lines of a different DT40 heritage [28].

### 3.2. Frequency of surface IgM-loss and Vλ sequence changes in DT40 cre and *Brca1*-deficient derivatives

To assess the role of *Brca1* in *Ig* GC, fluctuation analysis of surface IgM-loss frequency was performed. Multiple independent cultures (12-24) of the DT40 cre *Brca1*-deficient lines were cultured in parallel with the *Brca1*-proficient parent line for 2 to 5 weeks. All DT40 cre and DT40 cre-derived lines described here were surface IgM-positive at the start of culture (Fig. 1D). Over time in culture, surface IgM-loss mutants accumulate as assayed by flow cytometry of cells stained with anti-chicken IgM antibody. This change in surface IgM is an indicator of genetic changes occurring at *Ig* loci. The percentage of cells that lost surface IgM in each independent culture is plotted in Figure 2, in addition to the median IgM-loss frequency of each population. At two and four-week time points, the median IgM-loss frequency of the DT40 cre population was 0.4% and 0.9%, respectively. In comparison, *Brca1*-deficient cultures accumulated an increased frequency of IgM-loss cells (2.4% at two weeks and 5.7-6.5% at four weeks), with an intermediate frequency exhibited by the *Brca1*-heterozygous line (1.2% at two weeks and 3.2% at four weeks, Fig. 2A).

At the end of the culture period, three to five clones that displayed significant, but variable (ie., median to high) frequency of IgM-loss were chosen to analyze for DNA sequence changes in *Vλ*. DNA was isolated either from the total pool of cells of a particular clone, or from IgM-cells of a particular clone isolated by fluorescence-activated cell sorting (FACS) in order to analyze mutations in a 427-bp region of the rearranged *Vλ* gene of DT40. Sequence changes in *Vλ* were classified either as GCs derived from one (or more) of 25 available pseudo-*Vλ* donors } } or non-templated point mutations, as described [12]. Strikingly, whereas there were 5 times as many GCs as non-templated events in the *Brca1*<sup>+/+</sup> line, this disparity was reversed in the *Brca1*<sup>-/-</sup> line which showed 1 GC to about 4 non-templated events (Tables 2A and 2B). Despite the difference in type of mutation, mutations appear to be distributed similarly in *Brca1*-proficient and -deficient cells within the region of *Vλ* analyzed (Fig. 3). Although only very few non-templated mutations were found in DT40 cre, their point mutation pattern resembled that found in the *Brca1*-deficient derivatives, which were predominantly mutations from G and C (Fig. 2B). Mutation frequencies were  $0.43 \times 10^{-3}$  bp for DT40 cre and  $1.6 \times 10^{-3}$  bp for *Brca1*<sup>-/-</sup> derivatives.

### 3.3. Comparison of non-templated mutation patterns in *Brca1*- and XRCC3-deficient DT40

Fluctuation analysis of surface IgM-loss and sequence analysis of *Vλ* from 4-week cultured clones also was performed with *Brca1*-deficient lines derived independently from a DT40 parent (an IgM<sup>+</sup> clone derived from the CL18 line, [39] for which an XRCC3-deficient derivative was described previously [42]). As shown in Fig. 4A (Expt. #1), XRCC3-deficient DT40 accumulated IgM-loss variants at a significantly higher frequency than the XRCC3-proficient cells, as reported [12], whereas the median frequency of IgM-loss variants

accumulating in the *Brcal*-deficient lines was only slightly elevated. XRCC3-deficient cells also were tested in parallel with two independent *Brcal*-deficient derivatives of DT40 (both of which express no detectable *Brcal* protein, but which differ in that *Brcal*<sup>-/-</sup> “partial” was generated with the targeting vector depicted in Fig. 1, whereas the *Brcal*<sup>-/-</sup> “complete” used for most studies in this section, harbors a more extensive deletion of the *Brcal* locus, [39]. In comparison with the XRCC3<sup>-/-</sup> cultures, both *Brcal*<sup>-/-</sup> lines accumulated a significantly lower frequency of IgM-loss variants (Fig. 4A, Expt. #2). Sequence analysis of *V* $\lambda$  revealed that these *Brcal*-deficient DT40 accumulated mostly point mutations (albeit with a lower frequency despite a similar number of cell generations in culture), and very few GCs, like the XRCC3-deficient cells (Table 3A and 3B). The fact that both DT40 and DT40 *cre*-derived *Brcal*<sup>-/-</sup> cells accumulate non-templated point mutations largely in favor over GCs implicates *Brcal* specifically in Ig GC. The pattern of non-templated mutations in the XRCC3- and *Brcal*-deficient cells is similar (Fig. 4B), as is their distribution (Fig. S2).

Targeted hemizygous integration of *Brcal* partially reconstituted *Brcal* expression in DT40 *Brcal*<sup>-/-</sup> cells (Fig. S3). Sequence analysis of a small set of *Brcal*-rescued clones revealed a rescue of GC ability at the expense of untemplated mutations (Table 3A), suggesting restoration of *Brcal* function.

#### 3.4. Expression of AID, Rad6 and PCNA is not affected in DT40 cells lacking *Brcal*

To begin to address whether *Brcal* plays a direct or indirect role in Ig GC and the efficiency of non-templated point mutations, candidate genes encoding proteins with known or possible effects on Ig gene diversification were analyzed for expression in DT40 *Brcal*-deficient cells and controls. In microarray analyses, overexpression of *Brcal* in mammalian cells induced expression of *Rad6*, involved in regulating the error-free versus error-prone branches of DNA repair [43] and PCNA, the clamp that loads and holds DNA polymerases onto DNA. Ubiquitination of PCNA by the Rad6/Rad18 Ub ligase regulates the frequency of non-templated mutations in DT40 *V* $\lambda$  [44]. However, no change in transcript levels was detected by semi-quantitative RT-PCR for either PCNA or *Rad6* in *Brcal*-deficient DT40 cells (Figure 5).

#### 3.5. Aberrant genomic rearrangements involving the *V* $\lambda$ locus were not detectable either in *Brcal*-deficient, or XRCC3-deficient DT40

The increased ratio of non-templated point mutations to GCs in the *Brcal*- and XRCC3-deficient DT40 indicates that the favored outcome of AID-induced lesions toward GC in *V* $\lambda$  is perturbed. Absence of some DNA repair proteins (eg., ATM, NbsI, p53) results in AID-dependent chromosomal translocations involving *Ig V*- and *Ig S*-region DNA [45]. To investigate whether loss of *Brcal* could lead to *Ig V*-region translocations in DT40 too, we analyzed by Southern blotting the gross integrity of the *V* $\lambda$  locus in DT40 and derivatives lacking *Brcal* or XRCC3. As reported previously, individual CL18 and XRCC3-deficient clones after 5 weeks of passage all retained the expected genomic fragments following digestion with *Bam*HI/*Sal*I and a *V* $\lambda$ - promoter probe (Fig. S4). Similarly, in DT40*cre* and DT40*cre Brcal*<sup>-/-</sup> clones, no aberrant banding pattern was observed in DNA derived from 3-week old cultures (Fig. S5).

Genomic translocations might cause a growth disadvantage in long-term culture. Therefore, we also analyzed *V* $\lambda$  DNA in larger, multiply-passaged cultures from which individual clones were obtained by limiting dilution and passed for only one week (long enough to accumulate enough cells for Southern blotting). Again, no aberrant banding patterns associated with the *V* $\lambda$  locus were observed (Fig. S6). Therefore, genomic translocations involving the *V* $\lambda$  locus in DT40 and *Brcal*<sup>-/-</sup> derivatives may not be an outcome of aberrant processing of AID-induced lesions, or if they occur, they occur at a frequency of <2.13%.

## 4. Discussion

*Brc1* is a DNA repair protein that participates in many cellular processes [24]. The precise role of *Brc1* in these processes is undefined, but irreplaceable. At least one mechanism that might explain the cancer predisposition is the genomic instability conferred by loss of *Brc1* function. *Brc1* is reported to be involved in several pathways of DNA repair, particularly homologous recombination [28,29,46]. The results presented here implicate *Brc1* also in *Ig* GC. *Brc1*-deficiency in three independent lines of DT40 results in a shift in *V $\lambda$*  diversification from GC to point mutation, substantiating the role of *Brc1* in homologous recombination paths of DNA repair, and indicating a role for *Brc1* in AID-initiated DNA mutation. This *Brc1*<sup>-/-</sup> phenotype is similar to cells mutant for *Brc2*, or deficient for one of the Rad51 paralogs [12,15]. Whether the role of *Brc1* in *Ig* GC is direct or indirect is unknown. Expression of two genes (ie., *Rad6* and *PCNA*) involved in DT40 *Ig* gene diversification is not affected by loss of *Brc1*. *Brc1* is known to recruit Rad51 to DNA damage-induced nuclear foci [26,28,47] a function likely to be important for facilitating GC at *Ig* loci. Interestingly, *Brc1* fails to localize significantly at AID-initiated S-region DNA breaks in murine B cells induced for switch recombination [48]. However, whether *Brc1* is involved in CSR, a homology-independent, region-specific recombination mechanism, is unknown; homozygous *Brc1* deletion is lethal in mice.

Repair of an *I-SceI* site-specific DSB by homologous recombination is impaired significantly in DT40 cells lacking *Brc1* [30]. DSBs are thought to be repaired mainly by either of two pathways: faithfully by homologous recombination with an intact DNA sequence donor (eg., a sister chromatid in S and G2 phases of the cell cycle), or by NHEJ that ligates double-stranded DNA ends with little or no regard for sequence homology of the participating DNAs [49], reviewed by [50]. *Brc1* is reported also to regulate the fidelity of NHEJ by preventing DNA end resection that might otherwise result in extensive deletions [51,52]. We did not observe more, or larger, *V $\lambda$*  deletions in subclones of *Brc1*<sup>-/-</sup> DT40 as compared with controls, suggesting that in DT40 *Ig* gene diversification, *Brc1* plays no role in NHEJ and/or that a DSB is not an intermediate.

That *Ig* GC involving *Brc1* is initiated by a single-strand gap is an attractive possibility (see [53] and references therein), especially considering that the frequency of AID deamination is estimated to be too low in *V $\lambda$*  to initiate simultaneous deamination, Ung U-glycosylation, and abasic site nicking within a few bps on opposite strands to generate a DSB, as estimated to be too low in *V $\lambda$*  in DT40 cells lacking Ung or the pseudo *V $\lambda$*  genes [16,17,54]. Single-strand nicks could be converted to DSBs by a passing replication fork, but the fact that Ku70-deficiency has little [55,56] to no (our unpublished findings) apparent effect on the frequency of *Ig* GC in DT40 encourages the idea that single-strand gaps may be candidates for initiating *Ig* GC.

The shift toward favoring non-templated point mutations over GCs due to *Brc1*-deficiency is similar to the effect of deficiency of the Rad51 paralogs and *Brc2*. However, although the frequency of *V $\lambda$*  point mutations in *Brc1*<sup>-/-</sup> cells is elevated with respect to the *Brc1*-proficient control, they are not elevated to the level observed in XRCC3- deficient cells (Fig. 4, Table 3 and [12]). The pattern and distribution of non-templated mutations is similar in *Brc1*<sup>-/-</sup> and XRCC3<sup>-/-</sup> cells, suggesting that the fundamental mechanisms by which non-templated mutations are generated in *Ig* genes of DT40 cells are similar in the absence of *Brc1* or other homologous recombination factors, as well as in the absence of pseudo-gene donor sequence. Non-templated point mutations in DT40 *Ig* genes appear to be generated by a mechanism(s) analogous to that of SHM in mammals (though perhaps using different translesion polymerases); at the very least, these mechanisms are linked by their dependence on AID, Ung and Rev1 [19,20,57]. This study and others in DT40 reveal no defect in non-templated mutation



in DT40 lacking Brca1, Brca2, nor any of the Rad51 paralogs. Therefore these proteins probably are not required for bona fide mammalian SHM, but may regulate (i) the occurrence of SHM rather than genomic translocation or recombination, and (ii) SHM frequency (based on the difference in frequency of non-templated mutation accumulation in Brca1 versus XRCC3; see further below).

Ung-deficient DT40 produce only C to T (G to A) point mutations in  $V\lambda$  at a frequency that likely represents the approximate frequency of AID deaminations in  $V\lambda$  e.g., Ref. [17]. This mutation frequency is lower than that of the XRCC2-deficient cells [54]. One interpretation of this observation is that some AID-induced damage is restored to the original  $V\lambda$  sequence via XRCC2-mediated homologous recombination, for instance with a sister chromatid [54], or with pseudo- $V\lambda$  sequence that is identical with the active  $V\lambda$  locus sequence. The latter is supported by the report that deletion of the pseudo- $V\lambda$  genes in the DT40 $cre$  line causes a 2.5-fold higher mutation rate than XRCC3-deficiency in the same DT40 cell line [16]. Thus, since Brca1 deficiency increases non-templated mutations, Brca1 also would be implicated in repairing some AID-induced lesions by error-free recombination with pseudo- $V\lambda$  sequences. In addition, processing of the deaminated C to an abasic site by Ung, and perhaps further to a DNA strand break by enzymes able to nick at abasic sites, might facilitate an increase in the mutation rate by creating a substrate(s) for translesion polymerases when recombination is unavailable, or prevented. Translesion polymerases then would have the potential to generate additional point mutations beyond those introduced by AID alone. The degree to which translesion polymerases gain access might therefore regulate the frequency of mutation. For instance, XRCC2- and XRCC3-deficiency might stall homologous recombination early enough (though later than deletion of the pseudo- $V$  recombination donor sequence) to promote frequent translesion polymerase access; in contrast, Brca1-deficiency might stall replication intermediates later, at a stage less favorable for access by translesion polymerases. In support of this idea, DT40 lacking Rad54, which has a number of activities thought to contribute to homologous recombination including late-acting functions in filament disassembly [58] and Holliday junction migration [59], are defective for GC, but do not accumulate non-templated point mutations [60]. A similar defect occurs in DT40 cells lacking either FancC or FancD2, whose functions in DNA repair are unknown [35,37].

A key event in activating the Fanconi anemia (FA) DNA repair pathway is ubiquitination of FancD2, which results in relocalization FancD2 to chromatin (reviewed by [36]). Although ubiquitination of FancD2 occurs independently of Brca1 [61], Brca1 is required to recruit ubiquitinated FancD2 to DNA damage [61,62]. Because FancD2- and FancC-deficient DT40 are impaired for both *Ig* GC and non-templated mutations, one hypothesis for the role of these proteins would be that they promote both homologous recombination and translesion synthesis pathways (eg, [63]). According to this idea, absence of Brca1 would lead to failure of FancD2 recruitment, and therefore a reduced frequency relative to the Brca1-proficient control of both GC and point mutations, similar to FancD2 $^{-/-}$  and FancC $^{-/-}$  DT40. This we did not observe. Perhaps the role of Brca1 in *Ig* gene diversification is independent of FancD2/C, or possibly, the absence of Brca1 still allows hampered, or transient recruitment, of FancD2 to AID-induced lesions, allowing some repair. This would explain the lower frequency of non-templated mutations in Brca1- versus XRCC2-, XRCC3-deficient cells.

Finally, because Brca1-deficiency affects the type (ie., point mutation versus GC) of mutation in  $V\lambda$ , mutations that all are initiated by AID, Brca1 regulation of AID/Ung-generated DNA lesion repair is implied. In humans and mice, AID-initiated lesions have the potential to generate translocations. In human lymphomas with cell surface markers characteristic of germinal center activated B cells (eg., Hodgkin's lymphoma), translocations between *c-myc* and *IgH* S-regions, and occasionally in V-regions, are hallmarks [64]. Similarly, some translocations in murine B cell lymphomas between *IgH* loci and *c-myc* are AID- and Ung-

dependent, and their frequency is elevated in murine activated B cells that lack DNA repair factors including ATM, Nbs1 and p53 [45]. As such, AID-dependent DNA breaks, and perhaps downstream DNA intermediates of SHM, CSR and Ig GC, seem to be substrates for at least four pathways (i) somatic point mutation, generally thought to be achieved by error-prone DNA synthesis; (ii) CSR resulting from AID-dependent breaks that are joined to accomplish deletion of DNA between activated S-regions, and fusion of the V<sub>H</sub>-region to the switched C isotype; (iii) Ig GC that uses AID-dependent DNA breaks to initiate Ig GC; and (iv) inappropriate translocation of Ig gene sequence to another chromosome. The first three paths are developmentally programmed, and somehow regulated to achieve co-opting of proteins that normally would repair DNA, into processes that generate mutations. The fourth represents the canonical view of DNA repair -- to prevent genomic instability. Although Brca1 is involved in Ig GC, in mammals Brca1 may be crucial to the fourth pathway to prevent aberrant, non-regulated processing of AID-induced DNA breaks in activated B cells or other cells, a likely possibility given that many of the DNA repair proteins involved in CSR like Nbs1, Msh2, and ATM also regulate and/or interact with Brca1, and in fact may be regulated by Brca1 [51]. We did not observe an increase in translocations involving V $\lambda$  in *Brca1*<sup>-/-</sup> DT40, but V $\lambda$  translocations may be too rare. Checking for popular known translocations in mammalian cells deficient for Brca1 awaits a model system for depleting Brca1 in activated B cells.

## Supplementary Material

Refer to Web version on PubMed Central for supplementary material.

### Acknowledgements

We thank S. Takeda for CL18 and *XRCC3*<sup>-/-</sup> derivative thereof; H. Arakawa and J.-M. Buerstedde (via M. Nussenzweig and N. Papavasiliou) for DT40<sup>cre</sup> and the *AID*<sup>-/-</sup> derivative; N. Lowndes for anti Brca1 antibodies. We are grateful to O. Yildiz for help in vector construction and B. Buikema and C. Hall of the University of Chicago Sequencing Facility for excellent technical assistance. We gratefully acknowledge support by the University of Chicago Cancer Research Center for the use of the DNA Sequencing and Flow Cytometry Facilities. This work was supported by NIH grants AI47380 and AI053130 to U.S.

## References

1. Reynaud CA, Anquez V, Dahan A, Weill JC. A single rearrangement event generates most of the chicken immunoglobulin light chain diversity. *Cell* 1985;40:283–291. [PubMed: 3917859]
2. Reynaud CA, Anquez V, Grimal H, Weill JC. A hyperconversion mechanism generates the chicken light chain preimmune repertoire. *Cell* 1987;48:379–388. [PubMed: 3100050]
3. Reynaud CA, Dahan A, Anquez V, Weill JC. Somatic hyperconversion diversifies the single V<sub>H</sub> gene of the chicken with a high incidence in the D region. *Cell* 1989;59:171–183. [PubMed: 2507167]
4. Muramatsu M, Sankaranand VS, Anant S, Sugai M, Kinoshita K, Davidson NO, Honjo T. Specific expression of activation-induced cytidine deaminase (AID), a novel member of the RNA-editing deaminase family in germinal center B cells. *J Biol Chem* 1999;274:18470–18476. [PubMed: 10373455]
5. Withers DR, Davison TF, Young JR. Developmentally programmed expression of AID in chicken B cells. *Dev Comp Immunol* 2005;29:651–662. [PubMed: 15784295]
6. Di Noia J, Neuberger MS. Altering the pathway of immunoglobulin hypermutation by inhibiting uracil-DNA glycosylase. *Nature* 2002;419:43–48. [PubMed: 12214226]
7. Rada C, Williams GT, Nilsen H, Barnes DE, Lindahl T, Neuberger MS. Immunoglobulin isotype switching is inhibited and somatic hypermutation perturbed in UNG-deficient mice. *Curr Biol* 2002;12:1748–1755. [PubMed: 12401169]
8. Longerich S, Basu U, Alt F, Storb U. AID in somatic hypermutation and class switch recombination. *Curr Opin Immunol* 2006;18:164–174. [PubMed: 16464563]

9. Ramiro A, San-Martin BR, McBride K, Jankovic M, Barreto V, Nussenzweig A, Nussenzweig MC. The role of activation-induced deaminase in antibody diversification and chromosome translocations. *Adv Immunol* 2007;94:75–107. [PubMed: 17560272]
10. Buerstedde JM, Reynaud CA, Humphries EH, Olson W, Ewert DL, Weill JC. Light chain gene conversion continues at high rate in an ALV-induced cell line. *Embo J* 1990;9:921–927. [PubMed: 2155784]
11. Buerstedde JM, Takeda S. Increased ratio of targeted to random integration after transfection of chicken B cell lines. *Cell* 1991;67:179–188. [PubMed: 1913816]
12. Sale JE, Calandrini DM, Takata M, Takeda S, Neuberger MS. Ablation of XRCC2/3 transforms immunoglobulin V gene conversion into somatic hypermutation. *Nature* 2001;412:921–926. [PubMed: 11528482]
13. West SC. Molecular views of recombination proteins and their control. *Nat Rev Mol Cell Biol* 2003;4:435–445. [PubMed: 12778123]
14. Sonoda E, Sasaki MS, Buerstedde JM, Bezzubova O, Shinohara A, Ogawa H, Takata M, Yamaguchi-Iwai Y, Takeda S. Rad51-deficient vertebrate cells accumulate chromosomal breaks prior to cell death. *Embo J* 1998;17:598–608. [PubMed: 9430650]
15. Hatanaka A, Yamazoe M, Sale JE, Takata M, Yamamoto K, Kitao H, Sonoda E, Kikuchi K, Yonetani Y, Takeda S. Similar effects of Brca2 truncation and Rad51 paralog deficiency on immunoglobulin V gene diversification in DT40 cells support an early role for Rad51 paralogs in homologous recombination. *Mol Cell Biol* 2005;25:1124–1134. [PubMed: 15657438]
16. Arakawa H, Saribasak H, Buerstedde JM. Activation-induced cytidine deaminase initiates immunoglobulin gene conversion and hypermutation by a common intermediate. *PLoS Biol* 2004;2:E179. [PubMed: 15252444]
17. Saribasak H, Saribasak NN, Ipek FM, Ellwart JW, Arakawa H, Buerstedde JM. Uracil DNA glycosylase disruption blocks Ig gene conversion and induces transition mutations. *J Immunol* 2006;176:365–371. [PubMed: 16365429]
18. Guo C, Fischhaber PL, Luk-Paszyc MJ, Masuda Y, Zhou J, Kamiya K, Kisker C, Friedberg EC. Mouse Rev1 protein interacts with multiple DNA polymerases involved in translesion DNA synthesis. *Embo J* 2003;22:6621–6630. [PubMed: 14657033]
19. Ross AL, Sale JE. The catalytic activity of REV1 is employed during immunoglobulin gene diversification in DT40. *Mol Immunol* 2006;43:1587–1594. [PubMed: 16263170]
20. Simpson LJ, Sale JE. Rev1 is essential for DNA damage tolerance and non-templated immunoglobulin gene mutation in a vertebrate cell line. *Embo J* 2003;22:1654–1664. [PubMed: 12660171]
21. Yabuki M, Fujii MM, Maizels N. The MRE11-RAD50-NBS1 complex accelerates somatic hypermutation and gene conversion of immunoglobulin variable regions. *Nat Immunol* 2005;6:730–736. [PubMed: 15937485]
22. Neuberger MS, Harris RS, Di Noia J, Petersen-Mahrt SK. Immunity through DNA deamination. *Trends Biochem Sci* 2003;28:305–312. [PubMed: 12826402]
23. Antoniou A, Pharoah PD, Narod S, Risch HA, Eyfjord JE, Hopper JL, Loman N, Olsson H, Johannsson O, Borg A, Pasini B, Radice P, Manoukian S, Eccles DM, Tang N, Olah E, Anton-Culver H, Warner E, Lubinski J, Gronwald J, Gorski B, Tulinius H, Thorlacius S, Eerola H, Nevanlinna H, Syrjakoski K, Kallioniemi OP, Thompson D, Evans C, Peto J, Lalloo F, Evans DG, Easton DF. Average risks of breast and ovarian cancer associated with BRCA1 or BRCA2 mutations detected in case Series unselected for family history: a combined analysis of 22 studies. *Am J Hum Genet* 2003;72:1117–1130. [PubMed: 12677558]
24. Venkitaraman AR. Cancer susceptibility and the functions of BRCA1 and BRCA2. *Cell* 2002;108:171–182. [PubMed: 11832208]
25. Jasin M. Homologous repair of DNA damage and tumorigenesis: the BRCA connection. *Oncogene* 2002;21:8981–8993. [PubMed: 12483514]
26. Bhattacharyya A, Ear US, Koller BH, Weichselbaum RR, Bishop DK. The breast cancer susceptibility gene BRCA1 is required for subnuclear assembly of Rad51 and survival following treatment with the DNA cross-linking agent cisplatin. *J Biol Chem* 2000;275:23899–23903. [PubMed: 10843985]

27. Greenberg RA, Sobhian B, Pathania S, Cantor SB, Nakatani Y, Livingston DM. Multifactorial contributions to an acute DNA damage response by BRCA1/BARD1-containing complexes. *Genes Dev* 2006;20:34–46. [PubMed: 16391231]
28. Martin RW, Orelli BJ, Yamazoe M, Minn AJ, Takeda S, Bishop DK. RAD51 up-regulation bypasses BRCA1 function and is a common feature of BRCA1 deficient breast tumors. *Cancer Research*. 2007;In press
29. Moynahan ME, Chiu JW, Koller BH, Jasin M. Brca1 controls homology-directed DNA repair. *Mol Cell* 1999;4:511–518. [PubMed: 10549283]
30. Bridge WL, Vandenberg CJ, Franklin RJ, Hiom K. The BRIP1 helicase functions independently of BRCA1 in the Fanconi anemia pathway for DNA crosslink repair. *Nat Genet* 2005;37:953–957. [PubMed: 16116421]
31. Venkitaraman AR. Tracing the network connecting BRCA and Fanconi anaemia proteins. *Nat Rev Cancer* 2004;4:266–276. [PubMed: 15057286]
32. Chen J, Silver DP, Walpita D, Cantor SB, Gazdar AF, Tomlinson G, Couch FJ, Weber BL, Ashley T, Livingston DM, Scully R. Stable interaction between the products of the BRCA1 and BRCA2 tumor suppressor genes in mitotic and meiotic cells. *Mol Cell* 1998;2:317–328. [PubMed: 9774970]
33. Zhong Q, Chen CF, Li S, Chen Y, Wang CC, Xiao J, Chen PL, Sharp ZD, Lee WH. Association of BRCA1 with the hRad50-hMre11-p95 complex and the DNA damage response. *Science* 1999;285:747–750. [PubMed: 10426999]
34. Wang Q, Zhang H, Guerrette S, Chen J, Mazurek A, Wilson T, Slupianek A, Skorski T, Fishel R, Greene MI. Adenosine nucleotide modulates the physical interaction between hMSH2 and BRCA1. *Oncogene* 2001;20:4640–4649. [PubMed: 11498787]
35. Yamamoto K, Hirano S, Ishiai M, Morishima K, Kitao H, Namikoshi K, Kimura M, Matsushita N, Arakawa H, Buerstedde JM, Komatsu K, Thompson LH, Takata M. Fanconi anemia protein FANCD2 promotes immunoglobulin gene conversion and DNA repair through a mechanism related to homologous recombination. *Mol Cell Biol* 2005;25:34–43. [PubMed: 15601828]
36. Niedernhofer LJ, Lalai AS, Hoeijmakers JH. Fanconi anemia (cross)linked to DNA repair. *Cell* 2005;123:1191–1198. [PubMed: 16377561]
37. Niedzwiedz W, Mosedale G, Johnson M, Ong CY, Pace P, Patel KJ. The Fanconi anaemia gene FANCC promotes homologous recombination and error-prone DNA repair. *Mol Cell* 2004;15:607–620. [PubMed: 15327776]
38. Arakawa H, Lodygin D, Buerstedde JM. Mutant loxP vectors for selectable marker recycle and conditional knock-outs. *BMC Biotechnol* 2001;1:7. [PubMed: 11591226]
39. Orelli, BJ. The Division of the Biological Sciences and the Pritzker School of Medicine. Committee on Cancer Biology. University of Chicago; Chicago: 2004. DT40 cells as a model for the role of Brca1 in DNA repair.
40. McCormack WT, Hurley EA, Thompson CB. Germ line maintenance of the pseudogene donor pool for somatic immunoglobulin gene conversion in chickens. *Mol Cell Biol* 1993;13:821–830. [PubMed: 8423804]
41. Arakawa H, Hauschild J, Buerstedde JM. Requirement of the activation-induced deaminase (AID) gene for immunoglobulin gene conversion. *Science* 2002;295:1301–1306. [PubMed: 11847344]
42. Takata M, Sasaki MS, Tachiiri S, Fukushima T, Sonoda E, Schild D, Thompson LH, Takeda S. Chromosome instability and defective recombinational repair in knockout mutants of the five Rad51 paralogs. *Mol Cell Biol* 2001;21:2858–2866. [PubMed: 11283264]
43. Hoege C, Pfander B, Moldovan GL, Pyrowolakis G, Jentsch S. RAD6-dependent DNA repair is linked to modification of PCNA by ubiquitin and SUMO. *Nature* 2002;419:135–141. [PubMed: 12226657]
44. Arakawa H, Moldovan GL, Saribasak H, Saribasak NN, Jentsch S, Buerstedde JM. A role for PCNA ubiquitination in immunoglobulin hypermutation. *PLoS Biol* 2006;4:e366. [PubMed: 17105346]
45. Ramiro AR, Jankovic M, Callen E, Difilippantonio S, Chen HT, McBride KM, Eisenreich TR, Chen J, Dickins RA, Lowe SW, Nussenzweig A, Nussenzweig MC. Role of genomic instability and p53 in AID-induced c-myc-Igh translocations. *Nature* 2006;440:105–109. [PubMed: 16400328]
46. Snouwaert JN, Gowen LC, Latour AM, Mohn AR, Xiao A, DiBiase L, Koller BH. BRCA1 deficient embryonic stem cells display a decreased homologous recombination frequency and an increased

- frequency of non-homologous recombination that is corrected by expression of a *brca1* transgene. *Oncogene* 1999;18:7900–7907. [PubMed: 10630642]
47. Zhang J, Willers H, Feng Z, Ghosh JC, Kim S, Weaver DT, Chung JH, Powell SN, Xia F. Chk2 phosphorylation of BRCA1 regulates DNA double-strand break repair. *Mol Cell Biol* 2004;24:708–718. [PubMed: 14701743]
  48. Petersen S, Casellas R, Reina-San-Martin B, Chen HT, Difilippantonio MJ, Wilson PC, Hanitsch L, Celeste A, Muramatsu M, Pilch DR, Redon C, Ried T, Bonner WM, Honjo T, Nussenzweig MC, Nussenzweig A. AID is required to initiate Nbs1/gamma-H2AX focus formation and mutations at sites of class switching. *Nature* 2001;414:660–665. [PubMed: 11740565]
  49. Gu J, Lu H, Tippin B, Shimazaki N, Goodman MF, Lieber MR. XRCC4:DNA ligase IV can ligate incompatible DNA ends and can ligate across gaps. *Embo J* 2007;26:3506–3507.
  50. Lieber MR, Yu K, Raghavan SC. Roles of nonhomologous DNA end joining, V(D)J recombination, and class switch recombination in chromosomal translocations. *DNA Repair (Amst)* 2006;5:1234–1245. [PubMed: 16793349]
  51. Paull TT, Cortez D, Bowers B, Elledge SJ, Gellert M. Direct DNA binding by Brca1. *Proc Natl Acad Sci U S A* 2001;98:6086–6091. [PubMed: 11353843]
  52. Zhuang J, Zhang J, Willers H, Wang H, Chung JH, van Gent DC, Hallahan DE, Powell SN, Xia F. Checkpoint kinase 2-mediated phosphorylation of BRCA1 regulates the fidelity of nonhomologous end-joining. *Cancer Res* 2006;66:1401–1408. [PubMed: 16452195]
  53. Nagaraju G, Scully R. Minding the gap: the underground functions of BRCA1 and BRCA2 at stalled replication forks. *DNA Repair (Amst)* 2007;6:1018–1031. [PubMed: 17379580]
  54. Di Noia JM, Neuberger MS. Immunoglobulin gene conversion in chicken DT40 cells largely proceeds through an abasic site intermediate generated by excision of the uracil produced by AID-mediated deoxycytidine deamination. *Eur J Immunol* 2004;34:504–508. [PubMed: 14768055]
  55. Cook AJ, Raftery JM, Lau KK, Jessup A, Harris RS, Takeda S, Jolly CJ. DNA-dependent protein kinase inhibits AID-induced antibody gene conversion. *PLoS Biol* 2007;5:e80. [PubMed: 17355182]
  56. Tang ES, Martin A. NHEJ-deficient DT40 cells have increased levels of immunoglobulin gene conversion: evidence for a double strand break intermediate. *Nucleic Acids Res* 2006;34:6345–6351. [PubMed: 17142237]
  57. Jansen JG, Langerak P, Tsaalbi-Shtylik A, van den Berk P, Jacobs H, de Wind N. Strand-biased defect in C/G transversions in hypermutating immunoglobulin genes in Rev1-deficient mice. *J Exp Med* 2006;203:319–323. [PubMed: 16476771]
  58. Solinger JA, Kiiianitsa K, Heyer WD. Rad54, a Swi2/Snf2-like recombinational repair protein, disassembles Rad51:dsDNA filaments. *Mol Cell* 2002;10:1175–1188. [PubMed: 12453424]
  59. Bugreev DV, Mazina OM, Mazin AV. Rad54 protein promotes branch migration of Holliday junctions. *Nature* 2006;442:590–593. [PubMed: 16862129]
  60. Bezzubova O, Silbergleit A, Yamaguchi-Iwai Y, Takeda S, Buerstedde JM. Reduced X-ray resistance and homologous recombination frequencies in a RAD54<sup>-/-</sup> mutant of the chicken DT40 cell line. *Cell* 1997;89:185–193. [PubMed: 9108474]
  61. Vandenberg CJ, Gergely F, Ong CY, Pace P, Mallery DL, Hiom K, Patel KJ. BRCA1-independent ubiquitination of FANCD2. *Mol Cell* 2003;12:247–254. [PubMed: 12887909]
  62. Garcia-Higuera I, Taniguchi T, Ganesan S, Meyn MS, Timmers C, Hejna J, Grompe M, D'Andrea AD. Interaction of the Fanconi anemia proteins and BRCA1 in a common pathway. *Mol Cell* 2001;7:249–262. [PubMed: 11239454]
  63. Hinz JM, Nham PB, Salazar EP, Thompson LH. The Fanconi anemia pathway limits the severity of mutagenesis. *DNA Repair (Amst)* 2006;5:875–884. [PubMed: 16815103]
  64. Koppers R, Dalla-Favera R. Mechanisms of chromosomal translocations in B cell lymphomas. *Oncogene* 2001;20:5580–5594. [PubMed: 11607811]

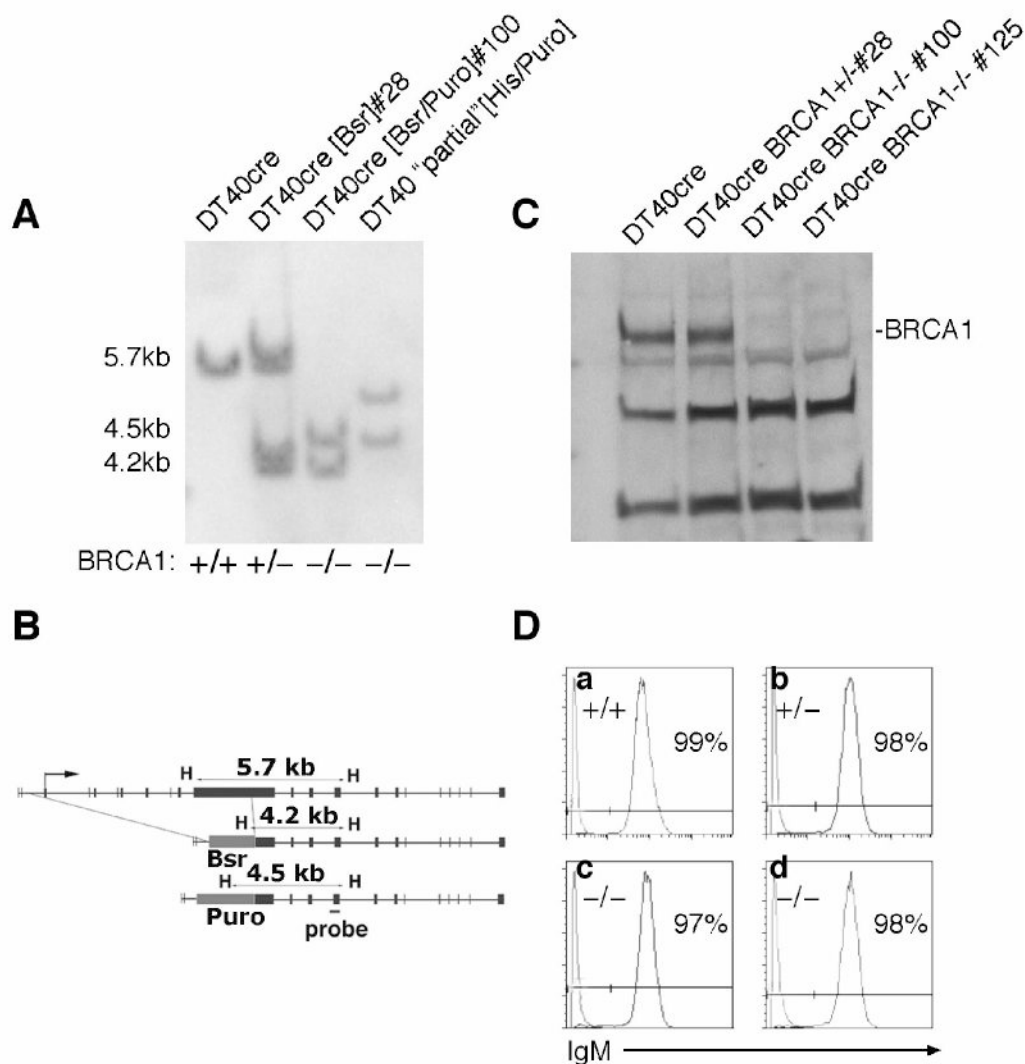


**Fig. 1.** *Brca1*-deficient derivatives of DT40 *cre*. (A) Southern blot. (B) Targeting strategy. (C) Western blot of nuclear lysates, blotted and probed with anti-serum to chicken *Brca1*. The position of *Brca1* is indicated. Other bands are non-specific proteins recognized by either the primary antiserum or secondary anti-rabbit IgG used for detection. (D) Flow cytometry of cells stained for surface IgM a – DT40 *cre* b – DT40 *cre* *Brca1*<sup>+/-</sup> c – DT40 *cre* *Brca1*<sup>-/-</sup> clone #100 d – DT40 *cre* *Brca1*<sup>-/-</sup> clone #125. One to two-week old cultures of each genotype were stained with anti-chicken IgM labeled with FITC, and analyzed by flow cytometry. All cultures are comprised of largely IgM<sup>+</sup> cells.

**Fig. 2A**

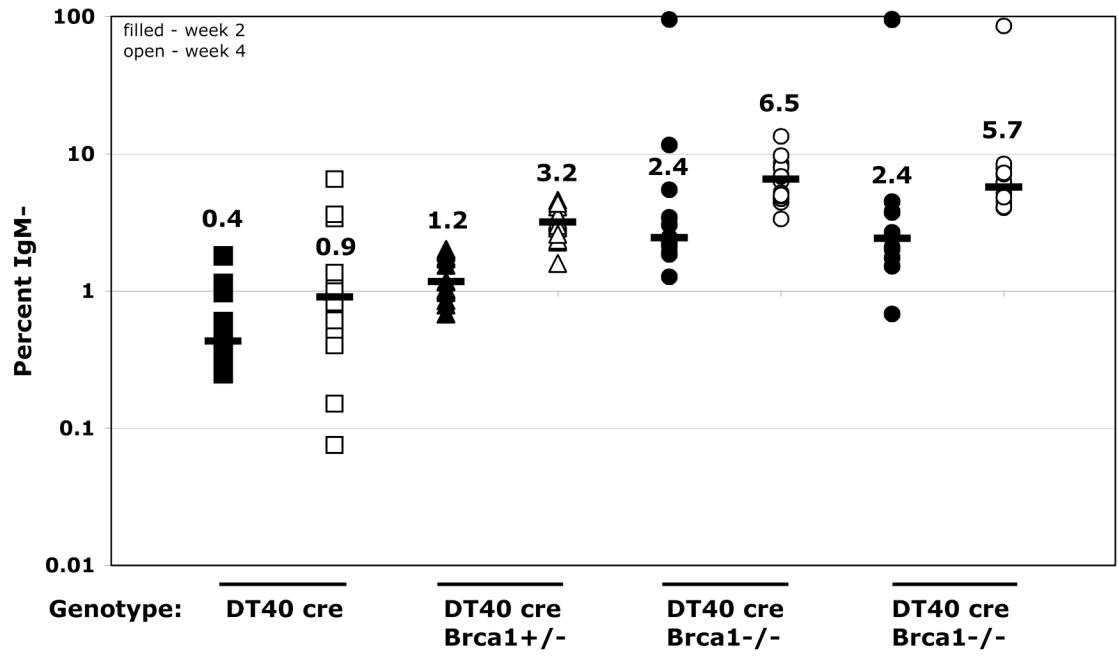


**Fig. 2B**

Selected for IgM-loss:

		to <b>DT40 cre</b>			
from		<b>A</b>	<b>C</b>	<b>G</b>	<b>T</b>
	<b>A</b>		0	0	0
	<b>C</b>	0		2	1
	<b>G</b>	0	0		0
	<b>T</b>	0	1	0	

		to <b>DT40 cre Brca1-/-</b>			
from		<b>A</b>	<b>C</b>	<b>G</b>	<b>T</b>
	<b>A</b>		0	0	0
	<b>C</b>	7		11	7
	<b>G</b>	3	10		6
	<b>T</b>	0	0	2	

Not selected:

		to <b>DT40 cre</b>			
from		<b>A</b>	<b>C</b>	<b>G</b>	<b>T</b>
	<b>A</b>		0	0	0
	<b>C</b>	1		3	3
	<b>G</b>	2	1		5
	<b>T</b>	0	0	0	

		to <b>DT40 cre Brca1-/-</b>			
from		<b>A</b>	<b>C</b>	<b>G</b>	<b>T</b>
	<b>A</b>		0	1	0
	<b>C</b>	10		45	21
	<b>G</b>	20	14		3
	<b>T</b>	1	2	1	

**Fig. 2.** Frequency of IgM loss and patterns of non-templated point mutations in V $\lambda$  in DT40 cre and derivatives deficient for Brca1. (A) Frequency of IgM loss. Each symbol represents the percentage of IgM-loss variants in an individual subclone after two (filled symbols) or four (open symbols) weeks of culture. The median percentage of IgM-loss of all subclones of a particular genotype is plotted as a large dash, with the value indicated above each set. (B) Patterns in V $\lambda$  of non-templated point mutations in cells of DT40 cre or Brca1-/- derivatives either selected, or not, for lack of surface IgM. Numbers are raw numbers of each class of base change.



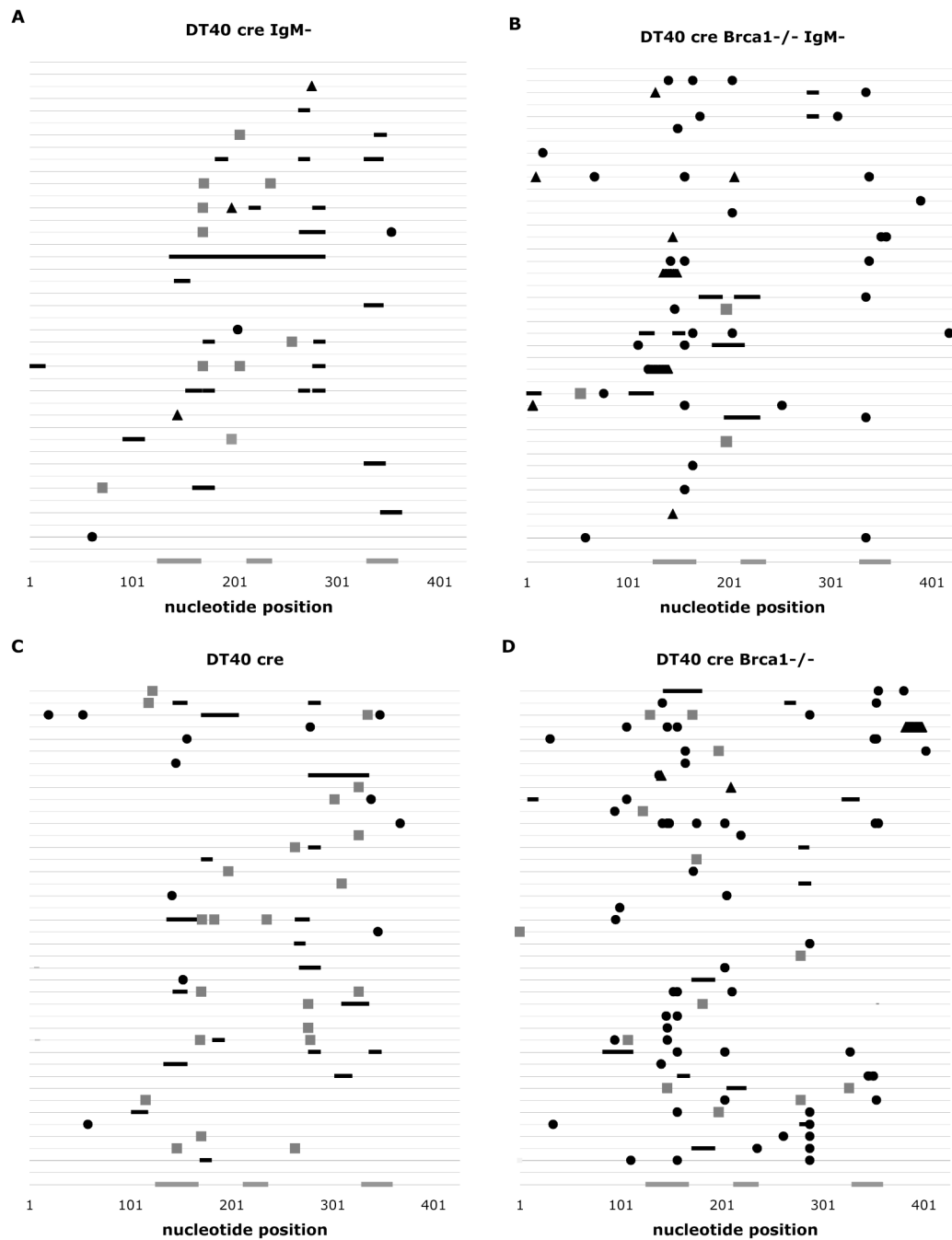


**Fig. 3.** Mutation distributions in randomly selected DT40 cre and Brca1-deficient derivatives. Each horizontal line is a map of events in one individual clone plotted with respect to the location in a 427-basepair region of *Vλ*. Nucleotide positions are indicated on the X-axis, and the three gray rectangles indicate the location of the three CDRs. Mutations from cells sorted for IgM loss are shown in plots (A) and (B), and from unsorted populations in plots (C) and (D). Filled circles represent non-templated point mutations, black lines represent gene conversions, filled trapezoids and triangles represent insertions and deletions, and gray squares are ambiguous events.

Fig. 4 A

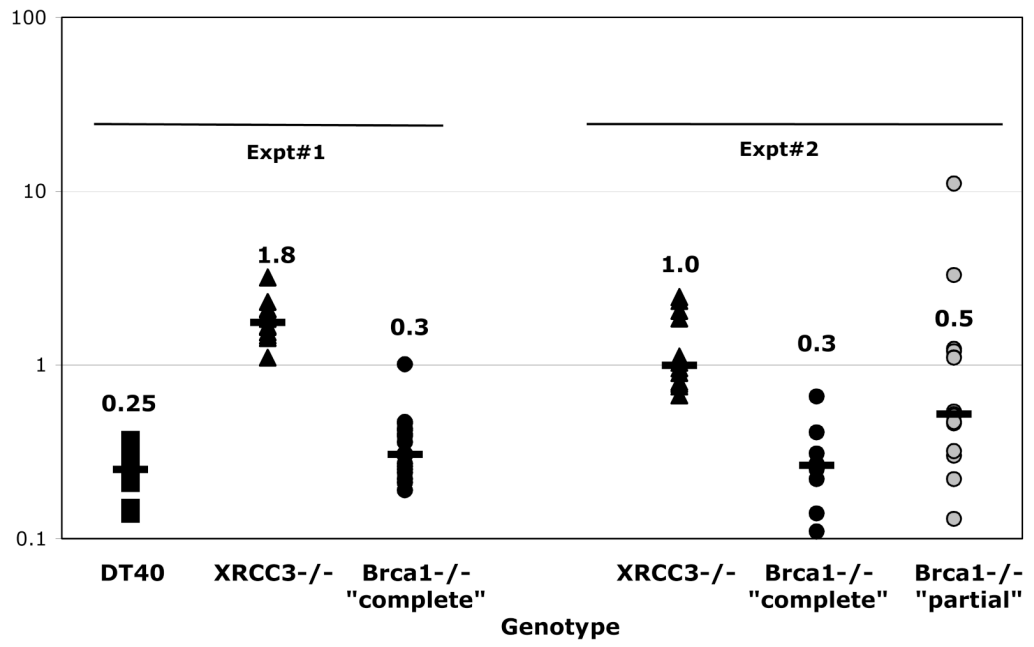


**Fig. 4B**

**Selected for IgM-loss:**

		to <i>Brca1</i> <sup>-/-</sup> (132)			
from		A	C	G	T
A			2(2)	1(1)	1(1)
C		15(11)		29(22)	20(15)
G		16(12)	30(23)		9(7)
T		0	7(5)	2(2)	

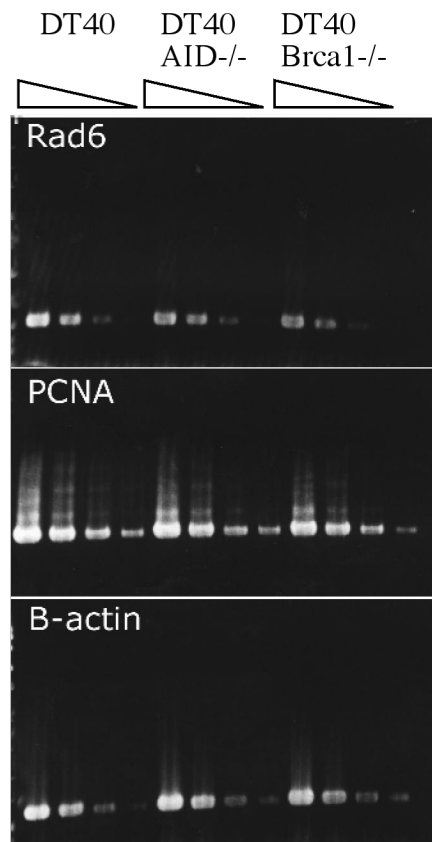
		to <i>XRCC3</i> <sup>-/-</sup> (110)			
from		A	C	G	T
A			0	1(1)	0
C		13(12)		33(30)	17(15)
G		19(17)	20(18)		8(7)
T		3(3)	1(1)	0	

**Not selected:**

		to <i>Brca1</i> <sup>-/-</sup> (32)			
from		A	C	G	T
A			0	1(3)	0
C		1(3)		12(38)	4(13)
G		7(22)	5(16)		0
T		1(3)	1(3)	0	

		to <i>XRCC3</i> <sup>-/-</sup> (41)			
from		A	C	G	T
A			0	0	0
C		2(5)		14(34)	12(29)
G		5(12)	6(15)		1(2)
T		0	1(2)	0	

**Fig. 4.** Frequency of IgM loss and mutation pattern in DT40 and derivatives deficient for XRCC3 or Brca1. (A) Frequency: Two independent experiments are shown. Each symbol represents the percentage of IgM-loss variants in an individual subclone after five weeks of culture. The median percentage of IgM-loss of all subclones of a particular genotype is plotted as a large dash, with the value indicated above each set. (B) Patterns of non-templated point mutations in Vλ, with or without selection for surface IgM phenotype. Raw numbers (% of total mutations).

**Figure 5 RT-PCR analysis of Rad6 and PCNA in DT40 cells deficient for Brca1**

**Figure 5.** RT-PCR analysis of Rad6 and PCNA in DT40 cells deficient for Brca1. As compared with the control gene,  $\beta$ -actin, no difference in expression of Rad6 and PCNA was observed in DT40 Brca1<sup>-/-</sup> cells. AID<sup>-/-</sup> cells are in the DT40 cre background and were used as an additional control.

**Table 1****Targeted integration frequencies for the *Brcal* locus in DT40 *cre***

Host cell	Selection-marker	Screened	Targeted
DT40 <i>cre</i>	blastidicin (Bsr)	41	4 (clone numbers 28, 29, 41 and 46)
DT40 <i>cre Brcal</i> +/- [Bsr] clone #41	puromycin	30	0
DT40 <i>cre Brcal</i> +/- [Bsr] clone #29	puromycin	75	0
DT40 <i>cre Brcal</i> +/- [Bsr] clone #46	puromycin	6	0
DT40 <i>cre Brcal</i> +/- [Bsr] clone #28	puromycin	139	3 (clone numbers 3, 100 and 125)

Table 2

Table 2A. Sequence changes in *V<sub>H</sub>* of IgM-loss variants from four-week cultures

Genotype	Gene conversion <sup>b</sup> (% of total events)	Non-templated point mutation <sup>c</sup> (% of total events)	Gene conversion:point mutation ratio <sup>d</sup>	Insertion/deletion/ duplication (% of total events)	Ambiguous <sup>e</sup> (% of total events)	Total events (# of sequenced clones)
DT40 <i>cre</i>	20 (53)	4 (11)	83:17	4 (11)	10 (27)	38 (46)
DT40 <i>cre Brca1</i> <sup>+/+</sup> (clone #28)	20 (48)	8 (19)	71:29	7 (17)	7 (17)	42 (36)
DT40 <i>cre Brca1</i> <sup>-/-</sup> (clones #100 and 125, pooled) <sup>a</sup>	11 (14)	46 (60)	19:81	14 (17)	6 (7)	77 (81)

Table 2B. Sequence changes in *V<sub>H</sub>* of four-week cultures, without selection for surface IgM phenotype

Genotype	Gene conversion (%) of total events)	Non-templated point mutation (% of total events)	Gene conversion:point mutation ratio	Insertion/deletion/ duplication (% of total events)	Ambiguous (% of total events)	Total events (# of sequenced clones)
DT40 <i>cre</i>	19 (26)	15 (21)	55:45	5 (7)	33 (46)	72 (187)
DT40 <i>cre Brca1</i> <sup>-/-</sup> (clones #100 and 125, pooled)	25 (12)	118 (59)	17:83	15 (7)	43 (21)	201 (286)

<sup>a</sup> Because the frequencies of IgM loss, gene conversion to point mutation ratios, point mutation pattern, and frequency of mutations was similar in the two independent *Brca1*<sup>-/-</sup> DT40 *cre* lines #100 and #125, data from the two clones were pooled.

<sup>b</sup> Sequence changes/events of two or more mutations were classified as a single gene conversion if they together matched a contiguous stretch of pseudo-*V<sub>H</sub>* gene sequence of  $\geq 9$  basepairs.

<sup>c</sup> Events were classified as non-templated point mutations if no matching stretch of  $\geq 9$  basepairs could be found in any pseudo-*V<sub>H</sub>* sequence.

<sup>d</sup> Expressed as a ratio of percents when total events are comprised only of gene conversions plus non-templated mutations.

<sup>e</sup> Single basepair mutations with no nearby mutations were classified as ambiguous if a stretch of  $\geq 9$  basepairs containing the change was present in pseudo-*V<sub>H</sub>* sequence.

**Table 3**  
**Patterns of mutation in V<sub>H</sub> of *Brca1*<sup>-/-</sup>, *XRCC3*<sup>-/-</sup> and *Brca1*-rescued DT40**

A Sequence changes in V<sub>H</sub>, without and without selection for surface IgM phenotype (all events pooled)

Genotype <sup>a</sup>	Gene conversion (% of total events)	Non-templated point mutation (% of total events)	Gene conversion: point mutation ratio	Insertion/deletion/ duplication (% of total events)	Ambiguous (% of total events)	Total events (# of sequenced clones)
<i>Brca1</i> <sup>-/-</sup> "complete" clone	11 (5)	166 (71)	6:94	28 (12)	29 (12)	234 (548)
<i>XRCC3</i> <sup>-/-</sup>	1 (12)	139 (59)	1:99	15 (7)	21 (21)	176 (277)
<i>Brca1</i> <sup>-/-</sup> "partial"	0	11 (58)	0:100	3 (16)	5 (26)	19 (68)
<i>Brca1</i> <sup>-/-</sup> ( <i>Brca1</i> knock-in rescue, clone F10)	6 (22)	12 (44)	33:67	3 (11)	6 (22)	27 (147)

**B Non-templated point mutation frequencies**

Genotype	Point mutations/total sequenced	IgM <sup>-</sup> sorted Point mutations/total sequenced	Mutation frequency <sup>b</sup>	Point mutations/total sequenced	Mutation frequency <sup>b</sup>
<i>Brca1</i> <sup>-/-</sup> "complete" clone	132/337		0.92 x 10 <sup>-3</sup>	32/211	0.36 x 10 <sup>-3</sup>
<i>XRCC3</i> <sup>-/-</sup>	110/136		1.9 x 10 <sup>-3</sup>	41/141	0.68 x 10 <sup>-3</sup>

<sup>a</sup> *Brca1*<sup>-/-</sup> "partial" is an independent clone with homozygous deficiency for *Brca1*, generated in the DT40 parent, with the same targeting vectors used to generate the *Brca1*-deficient DT40 *cre* derivatives. No *Brca1* protein is apparent in this line. The *Brca1*<sup>-/-</sup> "complete," clone 8, line has a more extensive deletion of the *Brca1* locus, and also makes no detectable *Brca1* protein. Numbers in table are raw numbers of each class (with all duplicated mutations from the same clone excluded to avoid resampling of the same mutations in a clonal lineage) followed in brackets by the percentage of the total in that class.

<sup>b</sup> Calculated as the number of point mutations per total basepairs sequenced (total clones sequenced times 427 – the length of V<sub>H</sub>, analyzed)